

Parametric seeding of a microresonator optical frequency comb

Scott B. Papp,* Pascal Del'Haye, and Scott A. Diddams

National Institute of Standards and Technology, Boulder, Colorado 80305, USA

[*scott.papp@nist.gov](mailto:scott.papp@nist.gov)

Abstract: We have investigated parametric seeding of a microresonator frequency comb (microcomb) by way of a pump laser with two electro-optic-modulation sidebands. We show that the pump-sideband spacing is precisely replicated throughout the microcomb's optical spectrum, and we demonstrate a record absolute line-spacing stability for microcombs of 1.6×10^{-13} at 1 s. The spectrum of a microcomb is complex, and often non-equidistant subcombs are observed. Our results demonstrate that parametric seeding can not only control the subcombs, but can lead to the generation of a strictly equidistant microcomb spectrum.

© 2013 Optical Society of America

OCIS codes: (190.4410) Nonlinear optics, parametric processes; (140.3948) Microcavity devices; (190.4380) Nonlinear optics, four-wave mixing.

References and links

1. V. Gerginov, C. E. Tanner, S. A. Diddams, A. Bartels, and L. Hollberg, "High-resolution spectroscopy with a femtosecond laser frequency comb," *Opt. Lett.* **30**, 1734–1736 (2005).
2. M. J. Thorpe, K. D. Moll, R. J. Jones, B. Safdi, and J. Ye, "Broadband cavity ringdown spectroscopy for sensitive and rapid molecular detection," *Science* **311**, 1595–1599 (2006).
3. T. Steinmetz, T. Wilken, C. Araujo-Hauck, R. Holzwarth, T. W. Hansch, L. Pasquini, A. Manescau, S. D'Odorico, M. T. Murphy, T. Kentscher, W. Schmidt, and T. Udem, "Laser frequency combs for astronomical observations," *Science* **321**, 1335–1337 (2008).
4. G. G. Ycas, F. Quinlan, S. A. Diddams, S. Osterman, S. Mahadevan, S. Redman, R. Terrien, L. Ramsey, C. F. Bender, B. Botzer, and S. Sigurdsson, "Demonstration of on-sky calibration of astronomical spectra using a 25 ghz near-ir laser frequency comb," *Opt. Express* **20**, 6631–6643 (2012).
5. P. Del'Haye, A. Schliesser, O. Arcizet, T. Wilken, R. Holzwarth, and T. J. Kippenberg, "Optical frequency comb generation from a monolithic microresonator," *Nature* **450**, 1214–1217 (2007).
6. A. A. Savchenkov, A. B. Matsko, V. S. Ilchenko, I. Solomatine, D. Seidel, and L. Maleki, "Tunable optical frequency comb with a crystalline whispering gallery mode resonator," *Phys. Rev. Lett.* **101**, 093902–4 (2008).
7. I. S. Grudin, N. Yu, and L. Maleki, "Generation of optical frequency combs with a CaF_2 resonator," *Opt. Lett.* **34**, 878–880 (2009).
8. S. B. Papp and S. A. Diddams, "Spectral and temporal characterization of a fused-quartz-microresonator optical frequency comb," *Phys. Rev. A* **84**, 053833– (2011).
9. S. B. Papp, P. Del'Haye, and S. A. Diddams, "Mechanical control of a microrod-resonator optical frequency comb," *PRX in press* and arXiv:1205.4272v1 (2012).
10. P. Del'Haye, S. B. Papp, and S. A. Diddams, "Hybrid electro-optically modulated microcombs," *Phys. Rev. Lett.* **109**, 263901– (2012).
11. J. Li, H. Lee, T. Chen, and K. J. Vahala, "Low-pump-power, low-phase-noise, and microwave to millimeter-wave repetition rate operation in microcombs," *Phys. Rev. Lett.* **109**, 233901– (2012).
12. J. S. Levy, A. Gondarenko, M. A. Foster, A. C. Turner-Foster, A. L. Gaeta, and M. Lipson, "Cmos-compatible multiple-wavelength oscillator for on-chip optical interconnects," *Nat Photon* **4**, 37–40 (2010).
13. A. A. Savchenkov, E. Rubiola, A. B. Matsko, V. S. Ilchenko, and L. Maleki, "Phase noise of whispering gallery photonic hyper-parametric microwave oscillators," *Opt. Express* **16**, 4130–4144 (2008).
14. P. Del'Haye, O. Arcizet, A. Schliesser, R. Holzwarth, and T. J. Kippenberg, "Full stabilization of a microresonator-based optical frequency comb," *Phys. Rev. Lett.* **101**, 053903–4 (2008).

15. P. Del'Haye, S. A. Diddams, and S. B. Papp, "Laser-machined ultra-high- Q microrod resonators for nonlinear optics," *Appl. Phys. Lett.* **102**, 221119–4 (2013).
16. F. Ferdous, H. Miao, D. E. Leaird, K. Srinivasan, J. Wang, L. Chen, L. T. Varghese, and A. M. Weiner, "Spectral line-by-line pulse shaping of on-chip microresonator frequency combs," *Nat Photon* **5**, 770–776 (2011).
17. T. Herr, V. Brasch, J. D. Jost, C. Y. Wang, N. M. Kondratiev, M. L. Gorodetsky, and T. J. Kippenberg, "Modelocking in an optical microresonator via soliton formation," arXiv:1211.0733 (2012).
18. K. Saha, Y. Okawachi, B. Shim, J. S. Levy, R. Salem, A. R. Johnson, M. A. Foster, M. R. E. Lamont, M. Lipson, and A. L. Gaeta, "Modelocking and femtosecond pulse generation in chip-based frequency combs," *Opt. Express* **21**, 1335–1343 (2013).
19. T. Herr, K. Hartinger, J. Riemensberger, W. C. Y., E. Gavartin, R. L. Holzwarth, M. Gorodetsky, and T. J. Kippenberg, "Universal formation dynamics and noise of kerr-frequency combs in microresonators," *Nat Photon* **6**, 480–487 (2012).
20. A. B. Matsko, A. A. Savchenkov, D. Strekalov, V. S. Ilchenko, and L. Maleki, "Optical hyperparametric oscillations in a whispering-gallery-mode resonator: Threshold and phase diffusion," *Phys. Rev. A* **71**, 033804–10 (2005).
21. Y. K. Chembo, D. V. Strekalov, and N. Yu, "Spectrum and dynamics of optical frequency combs generated with monolithic whispering gallery mode resonators," *Phys. Rev. Lett.* **104**, 103902–4 (2010).
22. H. Lee, T. Chen, J. Li, K. Y. Yang, S. Jeon, O. Painter, and K. J. Vahala, "Chemically etched ultrahigh- Q wedge-resonator on a silicon chip," *Nat Photon* **6**, 369–373 (2012).
23. M. Cai, O. Painter, and K. J. Vahala, "Observation of critical coupling in a fiber taper to a silica-microsphere whispering-gallery mode system," *Phys. Rev. Lett.* **85**, 74–77 (2000).
24. T. Carmon, L. Yang, and K. Vahala, "Dynamical thermal behavior and thermal self-stability of microcavities," *Opt. Express* **12**, 4742–4750 (2004).
25. D. V. Strekalov and N. Yu, "Generation of optical combs in a whispering gallery mode resonator from a bichromatic pump," *Phys. Rev. A* **79**, 041805–4 (2009).
26. J. Li, H. Lee, K. Y. Yang, and K. J. Vahala, "Sideband spectroscopy and dispersion measurement in microcavities," *Opt. Express* **20**, 26337–26344 (2012).
27. M. Kourogi, K. Nakagawa, and M. Ohtsu, "Wide-span optical frequency comb generator for accurate optical frequency difference measurement," *Quantum Electronics, IEEE Journal of* **29**, 2693–2701 (1993).
28. S. Xiao, L. Hollberg, and S. A. Diddams, "Generation of a 20 GHz train of subpicosecond pulses with a stabilized optical-frequency-comb generator," *Opt. Lett.* **34**, 85–87 (2009).
29. T. M. Fortier, M. S. Kirchner, F. Quinlan, J. Taylor, J. C. Bergquist, T. Rosenband, N. Lemke, A. Ludlow, Y. Jiang, C. W. Oates, and S. A. Diddams, "Generation of ultrastable microwaves via optical frequency division," *Nat. Photon.* **5**, 425 (2011).

The optical spectrum of a microresonator frequency comb (microcomb) is generated via parametric nonlinear optics, which can initiate with only milliwatts of CW pump laser power due to the high Q and small mode volume of microresonators. The simplicity of the generation mechanism, in combination with uniquely large line spacings in the 10's to 100's of GHz and the potential for photonic integration, makes microcombs a potential alternative for applications that currently rely on table-top combs. For example, applications such as direct spectroscopy [1], real-time trace detection [2], and astronomical spectrograph calibration [3, 4] call for robust, portable comb operation. The development of portable microcomb technology could also expand the reach of a comb's natural function, as an optical clockwork that leverages the remarkable precision of optical frequency measurements.

Microcomb generation has been studied with a range of microresonators from bulk devices such as microtoroids [5], crystalline resonators [6, 7], and microrods [8–10] to integration-capable platforms such as silica [11] and silicon nitride [12]. A common observation in microcomb experiments has been the lack of a deterministic modelocking mechanism, which enables the type of stable operation, equidistance of all comb lines, and ultrashort optical waveforms known from femtosecond modelocked lasers. Still, a number of interesting microcomb operating regimes have been reported including low-noise [9–11, 13–15], phaselocked [8, 16], and stabilized operation [9, 10, 14], and the generation of soliton waveforms [17, 18]. Theoretical models have been proposed that explain many microcomb behaviors [19–21]. But at present, a comprehensive picture of microcomb generation, and specifically a singular modelocking mechanism, have not been identified.

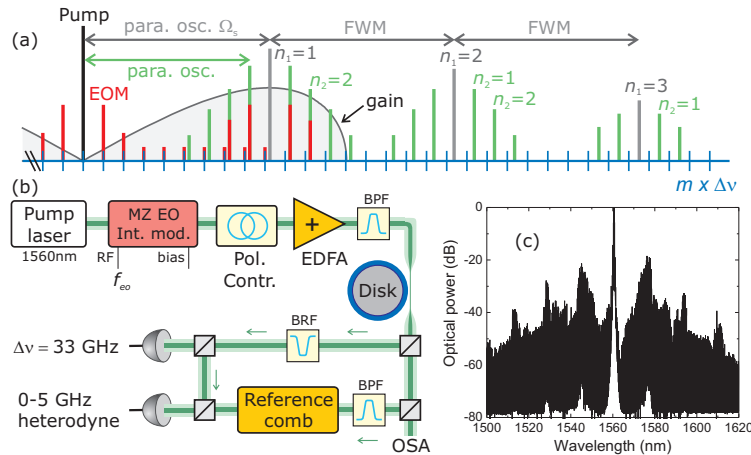


Fig. 1. Implementation of parametric seeding. (a) Model for comb generation based on parametric oscillation and FWM. A microcomb with a line spacing close to the resonator FSR is created via a primary parametric process (n_1) with spacing $\Omega_s \approx m_i \text{FSR}$ in combination with a secondary process (n_2) active in adjacent resonator modes. All other lines originate from these initial ones. Parametric seeding can influence comb generation not only by initiating the secondary process, but via injection seeding of the primary one. (b) The setup for our experiments consists of a laser, which is intensity modulated in a Mach-Zehnder EOM device, amplified, and coupled into a silica disk resonator [22] via tapered fiber [23]. To analyze microcomb spectra, we use photodetection to record the line spacing, and we make line-by-line optical frequency measurements with respect to a reference comb. BPF: bandpass filter, BRF: bandreject filter, OSA: optical spectrum analyzer. (c) Optical spectrum for a microcomb with parametric seeding.

This paper introduces a coherent control technique, *parametric seeding*, for microcombs by way of pump-laser electro-optic (EO) intensity modulation. When the seeding frequency (f_{eo}) is tuned close to the microresonator free-spectral range (FSR), the intensity modulation strongly influences the parametric nonlinear processes responsible for comb generation. We observe that the ~ 33 GHz line spacing (Δv) of the resulting microcomb spectrum is precisely locked to f_{eo} , and that Δv can be varied over a range of ~ 10 MHz, and we measure an absolute Δv stability of 1.6×10^{-13} at 1 s, which is consistent with state-of-the-art microwave oscillators. Furthermore, our parametric seeding technique enables systematic investigations of the microcomb generation process, specifically their non-equidistant “sub-comb” behavior first described in [19]. Finally, we demonstrate the emergence of a continuously equidistant microcomb spectrum tied to f_{eo} that results from amplification of the seeding input signal.

Figure 1(a) presents a simple model for microcomb generation, which is motivated by [19]. A CW pump laser (ω_p) excites one microresonator mode. At the threshold power for parametric oscillation, signal and idler waves are generated at a frequency offset from the pump laser of $\Omega_s \sim m_i \times \text{FSR}$, where m_i is an integer that counts by how many FSR the initial signal/idler pair are spaced from the pump. The frequency Ω_s is determined by the balance of phase mismatch from dispersion, nonlinear effects, and the resonator mode structure; Fig. 1(a) shows the basic shape of single-pump parametric gain for the material dispersion of fused silica. Without increased pump power, four-wave mixing (FWM) of pump, signal, and idler creates fields at $\omega_p + n_1 \Omega_s$ (gray lines), where the integer n_1 indicates the primary spacing. When pump power is increased, secondary parametric oscillation (often in resonator modes adjacent to the first signal/idler) and four-wave mixing occurs, leading to a comb spectrum (green lines) with line spacing close to the resonator FSR. Within the framework of this model the microcomb’s

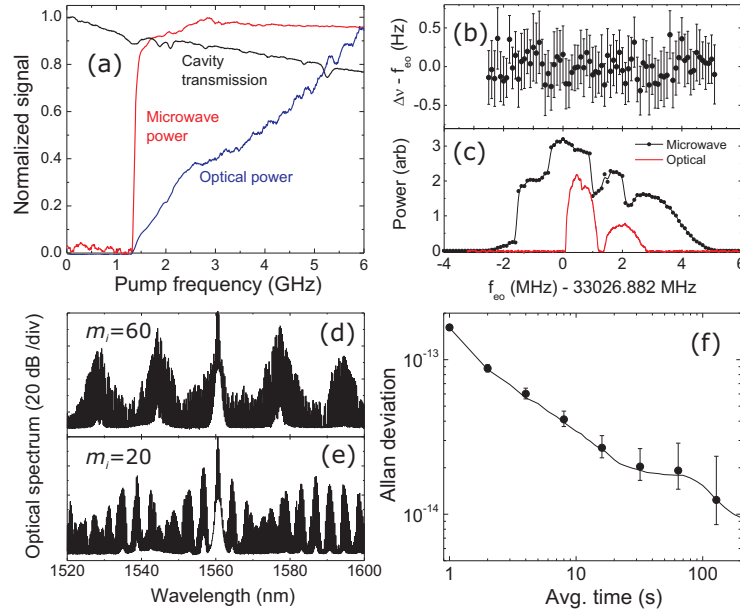


Fig. 2. Control of the microcomb line spacing via parametric seeding. (a) Disk resonator transmission with thermal bistability [24] (black), optical power (blue), and microwave power (red) as the pump laser is tuned onto resonance of the microcavity. The optical and microwave outputs of the comb are measured after filtering out the pump and sidebands. (b) Near-zero difference between the comb's line spacing ($\Delta\nu$) and seeding frequency (f_{eo}). (c) Optical (red) and microwave (points) power as f_{eo} is scanned. The resonator FSR is 33.02932(9) GHz. (d, e) Microcomb optical spectra for different settings of the seeding frequency; $f_{eo} = 33.026861$ in (d) and $f_{eo} = 33.030$ in (e). (f) Absolute line spacing Allan deviation as a function of measurement time.

spectrum is characterized by subcombs [19] that are written as

$$\nu_m = n_1 \Omega_s / 2\pi + n_2 \Delta\nu, \quad (1)$$

where ν_m is the frequency difference of $\omega_p/2\pi$ and the comb line, $m = n_1 m_i + n_2$ counts the mode number of the line relative to the pump, and n_1 (n_2) labels the order of the primary (secondary) parametric process. The spacing between most lines is $\Delta\nu$, but the comb is not equidistant since the parametric oscillation frequency $\Omega_s/2\pi$ is not required to be an integer multiple of $\Delta\nu$. Moreover, the subcomb lines “breathe” about the subcomb center, not the pump laser. This peculiar spectrum is different from a completely equidistant one with line number m separated from the pump laser by $\nu_m = m \Delta\nu$ (blue axis markers).

We expect parametric seeding with intensity modulation sidebands will impact microcomb generation in three ways. First, a few lines near the pump laser are created by way of FWM of the pump and sidebands. These lines are strictly equidistant from the pump laser due to energy conservation of FWM; such a bichromatic pump was explored in [25]. However, parametric gain near the pump is low, which limits the number and output power of these new comb lines. Second, pump intensity modulation creates sidebands of the parametric oscillation signal/idler waves at Ω_s . Since parametric gain is largest near the first signal/idler pair, the modulation-induced sidebands near Ω_s can rapidly grow, and FWM creates many new comb components, which importantly are all spaced by f_{eo} . Often we observe that seeded microcombs are composed of multiple, overlapped subcombs that are not continuously equidistant. Sections

1 and 2 of this paper present a detailed investigation of line spacing and subcomb control via parametric seeding. Third, the equidistant series of lines that arise from pump-seed FWM in the microresonator can influence parametric oscillation at Ω_s , and at best can completely injection-lock the primary process. Section 3 explores the competition between the parametric oscillation and pump-seed FWM, and the emergence of continuously equidistant microcomb spectrum.

1. Control of microcomb line spacing via parametric seeding

A schematic of our system is shown in Fig. 1(b). To derive the parametric seeding signal, a CW laser's intensity is modulated at frequency f_{eo} with a standard Mach-Zehnder electro-optic modulator. The relative power of the carrier and seeding sidebands is controlled by a bias voltage, and is typically set to $> 10\%$ of the carrier. The second-order sidebands have 40 dB less power than the first-order ones. After amplification to a maximum of 140 mW, the light is coupled into a disk resonator using a tapered fiber. The 2 mm diameter, 8 μm thick silica disk resonator is fabricated on a silicon chip using the procedure described in [22]. The particular optical mode we use has $Q = 63 \times 10^6$ and offers among the widest comb span (~ 400 nm) observed with this device. By tuning the pump-laser frequency toward cavity resonance, we generate the gap-free optical spectrum shown in Fig. 1(b) that covers significantly more than 120 nm. We analyze the microcomb spectrum with two techniques: Direct photodetection to characterize the microwave line spacing, and by use of a reference comb (described below) to understand the frequency spacing between the pump and microcomb lines. For all of the data in this paper except optical spectra, the central 2 nm of the comb is blocked to study only microcomb lines generated inside the disk resonator.

Parametric seeding can significantly reduce the dramatic changes in optical and microwave outputs that are typically observed in single-pump microcombs [8]. Figure 2(a) shows how the total cavity transmission and thermal triangle (black line), integrated optical power (blue line), and integrated microwave power near 33 GHz (red line) of the comb evolve as the pump laser frequency is scanned. Importantly at the ~ 10 mW parametric threshold, both the optical and microwave power switch on. In contrast, without f_{eo} the line spacing at threshold would be $60 \times \text{FSR}$ and undetectable electronically. In addition, the optical and microwave power outputs are stabilized by the parametric seeding, and they grow smoothly as the pump frequency tunes toward the microcavity resonance.

By tuning the seeding frequency f_{eo} , different aspects of microcomb generation process can be explored. Specifically, we discovered that distinct microcomb operating regimes exist, but that the line spacing is always precisely f_{eo} . The red line in Fig. 2(c) shows the comb's optical power (central 2 nm about pump removed) as a function of f_{eo} . Here the pump power is maintained *below* parametric threshold, and the comb's output is zero unless f_{eo} is tuned close to modes adjacent to the pump. Qualitatively different combs are generated for f_{eo} settings only a few MHz apart: At $f_{eo} \lesssim 33.028$ GHz, the primary parametric process occurs at $m_i \approx 60$ modes from the pump, while at $f_{eo} \gtrsim 33.028$ GHz, the comb is characterized by the smaller primary spacing $m_i \approx 20$; and at the intermediate setting of $f_{eo} \approx 33.0282$ GHz no comb is generated. Parametric phase matching depends on numerous parameters, and is apparently influenced by the line spacing of the emergent comb. For reference, the resonator's FSR is 33.02932(9) GHz, which is measured at low power and calibrated with the modulation sidebands [11]. Also, the nonlinear Kerr shift is ~ 30 MHz, which indicates the amount of dispersion needed to phase match parametric oscillation. The dispersion of disk resonators is described in [26].

When we increase intracavity power to above parametric threshold, the clean distinction between the two regimes is lost. The black points in Fig. 2(c) show the complicated dependence of microwave output power on f_{eo} . At the high and low f_{eo} frequency tails of microwave power, we observe combs with either $m_i \approx 60$ or $m_i \approx 20$; the optical spectra of these cases (Fig. 2(d) and (e)) clearly show the different primary spacings. But in between these extremes is a

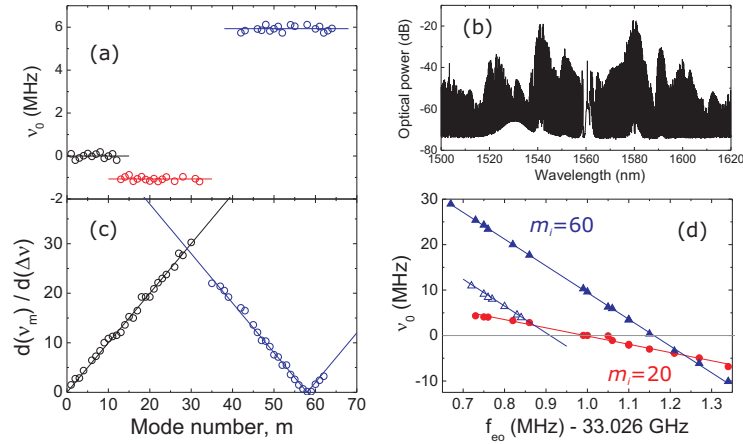


Fig. 3. Subcomb behavior in microcombs. (a) Line frequency diagram (v_0 vs. m) for a microcomb composed of three independent subcombs. The black points represent FWM of the pump and seeding sidebands, and the red (blue) points represent the $m_i \approx 20$ ($m_i \approx 60$) subcomb. (b) Optical spectrum with three subcombs. The pump laser and seeding sidebands are filtered out. (c) Comb line tuning rate versus m . Here f_{eo} is set so only the $m_i \approx 60$ subcomb is present. (d) Tuning of the independent subcomb offset frequencies with f_{eo} . For the open triangles, the pump laser frequency is adjusted to shift the v_0 of all the points.

transition region in which both m_i type combs are simultaneously possible. Still, as shown in Fig. 2(b), for every f_{eo} data point the Δv we measure (via frequency counting) is locked to f_{eo} within ± 0.5 Hz. Hence, no line-spacing stabilization post-generation is required. For a single f_{eo} setting, we measured the absolute Allan deviation of Δv by comparing it to an independent hydrogen maser reference; see Fig. 2(f). The 1.6×10^{-13} stability we achieve exceeds by 10x previous results obtained with microcombs [9]. To achieve 1 ms and longer stability beyond that of masers, we could reference the seeded microcomb to an optical clock via feedback to f_{eo} . However, it may be difficult to reduce the impact of wideband noise on the synthesizer that generates f_{eo} . We note that the measured absolute stability at 1 s is essentially the same as one would obtain by directly comparing the two independent masers. This implies that the residual noise, which represents the degree to which the parametrically-generated comb spacing tracks f_{eo} , would be significantly lower. This is consistent with other control techniques we have demonstrated [9, 10] where residual noise in the 10^{-15} range was achieved.

2. Optical frequency spectra of subcombs

Parametric seeding via intensity modulation has an impact not only on the microcomb line spacing, but also on the subcomb behavior described by Eqn. 1. Here we present an experimental study of how the optical frequency of microcomb lines depends on f_{eo} . Specifically, we demonstrate that the teeth of each subcomb breathe about the center of the subcomb, instead of the pumping laser, and that the subcomb offset from equidistance can be controlled with f_{eo} . Moreover, we identify a common behavior in microcomb generation, namely that a single microcomb tooth often has spectral contributions from independent subcombs.

To characterize the optical frequency spectrum of our microcomb, we derive a reference comb from the pump laser; see the schematic in Fig. 1(b). After exiting the disk microresonator and tapered fiber, the pump laser is separated from the rest of the microcomb spectrum with an optical filter. This pump light generates a comb covering 1540 nm to 1580 nm with 10 GHz spacing using a Fabry-Perot EO modulator [27, 28]. By photodetection of the interference be-

tween the microcomb and reference comb, we obtain a series of RF signals between zero and 5 GHz. Each RF signal is associated with a specific optical heterodyne beatnote between microcomb and reference lines. Using the two combs' precisely known line spacings, we determine the absolute difference between the pump and microcomb line (Eqn. 1), and the offset of the microcomb line from equidistance:

$$v_0 = v_m - m \Delta\nu = n_1 (\Omega_s/2\pi - \Delta\nu m_i). \quad (2)$$

Figure 3(a) shows v_0 versus microcomb mode number at $f_{eo} = 33.02706$ GHz. This microcomb line frequency diagram indicates the presence of three combs all with the same line spacing. (If the combs' spacing were not the same, then v_0 would vary with m .) One comb (black points) originates directly from FWM of the pump laser and modulation sidebands, hence it is strictly equidistant with offset -0.6 (120) kHz. But it is only composed of 13 lines near the pump. The other two subcombs have offsets of -1.06 MHz and 5.93 MHz from equidistance, and they originate from independent parametric oscillation processes with $m_i \approx 20$ (red points) and $m_i \approx 60$ (blue points), respectively. These data show that for this setting of f_{eo} , the microcomb operates in the transition between the two m_i regimes, and that multiple independent parametric processes are active. Fig. 3(b) shows a microcomb optical spectrum with two active subcombs.

We analyze how the subcomb lines breathe by varying the line spacing. First, we focus on settings of $f_{eo} \lesssim 33.0269$ GHz, for which the $m_i \approx 60$ subcomb is dominant. To measure the tuning rate $|\frac{d(v_m)}{d(\Delta\nu)}| = |n_2|$, we vary f_{eo} over a total range of 120 kHz and observe all the comb line frequencies for $m = \{0, 70\}$; Fig. 3(c) shows the tuning rate versus mode number. The blue points covering $m = \{35, 65\}$ have a tuning rate characteristic of the $n_1 = 1, m_i \approx 60$ subcomb, hence they have the expected $n_2 = m - m_i$ dependence given by the blue lines. This observation is strong evidence in support of the subcomb model, and future applications of microcombs could take advantage of the reduced sensitivity to $\Delta\nu$ of some lines. Conversely, the black points at small m result from FWM of the modulation sidebands and pump. The linear increase in tuning rate with m further confirms that these lines do not originate from a subcomb.

The subcomb offset frequency (Eqn. 2) also depends on the line spacing. Figure 3(d) shows v_0 obtained from line-frequency diagrams taken over a wide range of f_{eo} . Here both the $m_i \approx 20$ and $m_i \approx 60$ subcombs are excited. The subcomb offset frequency varies continuously through zero with a linear slope of $-m_i$ as f_{eo} changes. Unfortunately, the f_{eo} setting to realize $v_0 \simeq 0$ is different for the two subcombs. Here the ability to systematically vary v_0 is primarily due to control of $\Delta\nu$, as opposed to a more fundamental ability to influence the parametric phase-matching condition, which determines Ω_s . Hence, when we change the intracavity power via the pump-laser frequency [24], which is expected to modify Ω_s , we observe a shift in the $v_0 = 0$ intercept; see the open triangles in Fig. 3(d). However the underlying linear sensitivity of v_0 to f_{eo} is unchanged.

3. Emergence of a continuously equidistant microcomb

For precise optical frequency measurements, it would be beneficial to extend the offset-free series of lines that originates from pump-seed FWM throughout the entire microcomb spectrum, and to suppress subcomb generation. Here we demonstrate parametric amplification of the offset-free lines to at least microcomb mode 54 (± 1.8 THz from pump), conditioned on tuning the subcomb offset (v_0) close to zero. Such an equidistant comb appears even in the presence of the other $m_i \neq 0$ subcombs, which we described in Sec. 2. We interpret this behavior as incomplete injection locking of the subcombs by the parametric seeding. Interestingly, multiple lines, which compete for parametric gain, are observed in a single m -mode of the microcomb.

Figure 4(a) shows the optical heterodyne beat spectrum of the microcomb and reference comb for several m values. Here the frequency axis is precisely calibrated at the Hz level to

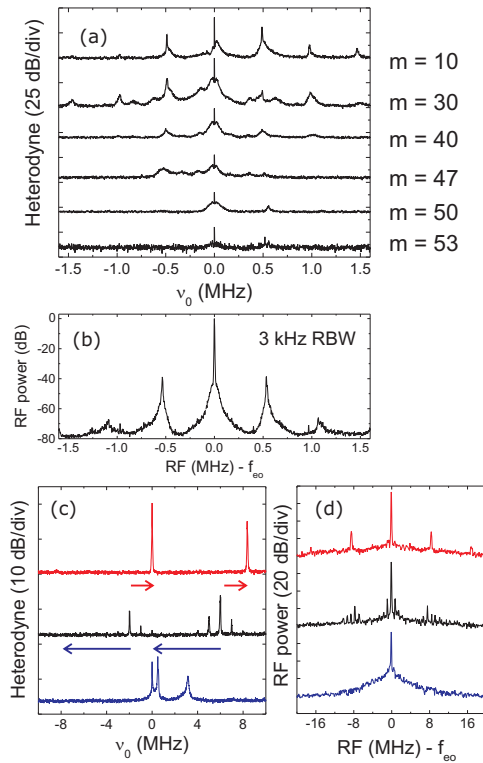


Fig. 4. Onset of a continuously equidistant microcomb. (a) Optical heterodyne of various microcomb m -lines and the reference comb. The narrow peak in each trace at ν_0 indicates the presence of an equidistant microcomb line, while the other peaks belong to the $m_i \approx 60$ subcomb. (b) Microcomb line spacing spectrum for data in (a). The equidistant and subcomb lines have the same spacing, but the subcomb offset appears here at ± 0.5 MHz. (c) Black trace is the optical heterodyne signal for microcomb line $m = 40$ showing the $n_1 = 2$, $m_i \approx 20$ subcomb at -2 MHz, and the $n_1 = 1$, $m_i \approx 60$ subcomb at 5 MHz. Apparently the microcomb's spectrum can consist of lines separated by more than the resonator's linewidth. Tuning the pump laser frequency by on order of ± 100 MHz shifts the subcomb lines' ν_0 . The upper (red) and lower (blue) traces show injection locking of the two subcombs, which is obtained by tuning their ν_0 toward zero. (d) Microwave output of the comb for the traces in (c).

represent ν_0 . Each trace is composed of several peaks, including a peak for the equidistant comb, a peak for the $m_i \approx 60$ subcomb, and their nonlinear mixing products. The peaks centered at $\nu_0 = 0$ have a narrow spectral width since pump laser frequency noise is common mode to both the equidistant microcomb and the reference comb. Moreover the ν_0 frequency of these peaks does not vary from zero when the pump frequency is tuned. These factors help significantly in identification of the equidistant comb. As expected, the ν_0 frequency of lines shown here, which belong to the $m_i \approx 60$ subcomb, do change with pump frequency.

The microwave line spacing spectrum we obtain via photodetection also provides information about the equidistant and offset microcomb components; see Fig. 4(b). Here the frequency axis covers the same range as in Fig. 4(a) to highlight their correspondence. This signal is composed of a strong peak at f_{eo} due to pairwise interference of adjacent lines among all the subcombs, and also of a series of peaks at multiples of 0.5 MHz from f_{eo} . Previous microcomb experiments identified these additional peaks in the line-spacing spectrum as interference

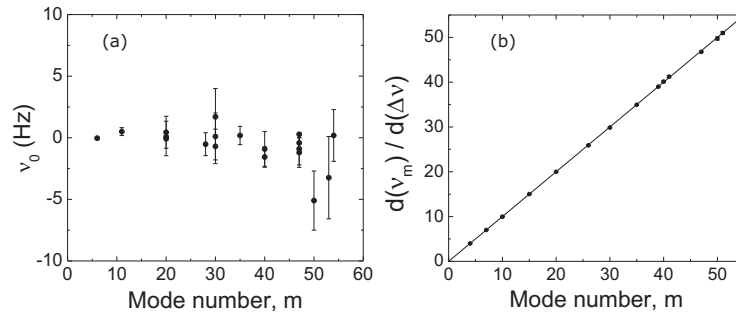


Fig. 5. Properties of the equidistant microcomb spectrum. (a) Measurements showing no offset from equidistance at the 2 Hz level for select m values up to 54. Error bars are the standard deviation of the mean for each point. (b) Equidistant comb line tuning versus m with slope of one.

of overlapping subcomb lines with, for example, $n_1 = 1$ and $n_2 = 2$ [19]. However, in our case they also clearly indicate the presence of a continuously equidistant microcomb spectrum among separate, offset subcombs. In fact, increasing the power in the additional peaks leads to a stronger equidistant comb.

We interpret the spectra in Fig. 4(a) and (b) as evidence for parametric-gain competition between different processes and partial injection locking of the subcombs. While the parametric-gain spectrum is extremely broad, signal/idler fields can only be efficiently created within the resonance spectrum of the optical microcavity. Naturally, to generate a completely equidistant comb the resonator modes must roughly line up with a fixed spacing; whereas for an offset subcomb, Ω_s of signal/idler fields changes with the resonator modes. Hence, a subcomb line provides a coarse marker of the resonator mode. For a fixed setting of f_{eo} , we explore the competition between parametric processes by varying the pump laser frequency. Fig. 4(c) shows heterodyne beatnote spectra of the $m = 40$ microcomb line with v_0 calibrated based on f_{eo} ; the three traces are different settings of the pump laser frequency, and in Fig. 4(d) are the corresponding line-spacing signals. The black trace (middle) demonstrates the complicated generation mechanism of microcombs: The peaks at positive (negative) v_0 originate from a $m_i \approx 60$ ($m_i \approx 20$) subcomb, and their ~ 1 MHz side peaks are associated with nonlinear mixing of their subcomb offset. For the black trace, the pump frequency is set such that the equidistant $m = 40$ line is between the two subcomb lines. All the characteristics of this optical heterodyne signal are mirrored in the line spacing spectrum we measure, namely peaks at $f_{eo} \pm 8$ MHz and ± 1 MHz corresponding to the subcomb offsets. Conversely, when we use the pump laser to tune the $m_i \approx 20$ line close to $v_0 = 0$ (upper, red trace), the $m = 40$ equidistant component is strongly amplified, the $m_i \approx 20$ subcomb component disappears, but the $m_i \approx 60$ subcomb remains. Tuning the pump frequency in the opposite direction (lower, blue trace) results in amplification of the equidistant line, reduction of the $m_i \approx 60$ subcomb, and complete disappearance of the $m_i \approx 20$ one. Again, the microwave line spacing spectra we obtain mirror the behavior of corresponding red and blue optical heterodyne traces.

Generating an equidistant spectrum is important for many future applications of microcombs, particularly ones that leverage frequency division from the optical to microwave domains [29]. To characterize its equidistance, we perform high-resolution measurements of the microcomb optical frequency spectrum using the reference comb. Here we use a microwave spectrum analyzer to repeatedly measure the microcomb-reference beat frequencies. Figure 5(a) shows measurements of v_0 for up to mode 54 from the pump laser. The offset we observe for all the studied m values is within the ~ 2 Hz uncertainty of our measurements. Specifically, for $m = 54$

the fractional uncertainty in our offset measurement is 1×10^{-12} . By varying f_{eo} and monitoring the frequency of each comb line, we characterize the tuning behavior of the equidistant comb; see Fig. 5(b). In contrast to the subcomb measurements presented in Sec. 2, the equidistant comb tunes precisely with the expected dependence on m . These data demonstrate that, even for the weak -60 dBm optical line powers of our reference comb, the equidistant microcomb we create is capable of precision optical frequency metrology across a significant fraction of its span. Moreover, generation of the equidistant comb is repeatable after switching the seeding and/or the entire microcomb system off and on.

4. Conclusion

In this paper, we have introduced a new parametric seeding technique for microcombs that provides for deterministic generation of the comb spectrum with known spacing. Our measurements of the absolute line-spacing stability reach a record level commensurate with state-of-the-art electronic oscillators. Moreover, the data in this paper demonstrate that parametric seeding is an important tool for understanding the generation of microcombs. Our simplified generation model (Fig. 1) is based on primary and secondary parametric oscillation processes, and we observe that at least three pairs of these processes can be active in creating a composite microcomb spectrum. Importantly, parametric seeding can influence all aspects of microcomb generation. We verified the dependence of subcomb lines on the microcomb's fundamental line spacing, and we demonstrated that subcomb offsets can be tuned through zero by changing the line spacing. However, simply tuning the subcomb offset to zero with $\Delta\nu$ does not necessarily yield the type of equidistant comb that will be important for future applications. On the other hand, even in the presence of multiple subcombs, we observe the emergence of a continuously equidistant spectrum that results from amplification of the parametric seeding signal, and we show that its offset from equidistance can be as low as 10^{-12} . Future experiments will focus on seeding with more than two sidebands, and on investigating \sim picosecond optical waveforms associated with the microcomb spectra presented here.

Acknowledgments

We are grateful to Hansuek Lee, Jiang Li, and Kerry Vahala for providing the silica disk resonator. We thank Lora Nugent-Glandorf and Frank Quinlan for providing helpful comments on this manuscript. This work is supported by the DARPA QuASAR program, NASA, and NIST. It is a contribution of the US government (NIST) and is not subject to copyright in the United States.